

## REFERENCES

- [1] H. F. Cooke, "Microwave FET's—A status report," in *IEEE ISSCC Dig. Tech. Papers*, 1978, pp. 116–117.
- [2] H. Rothe and W. Dahlke, "Theory of noisy fourpoles," *Proc. IRE*, vol. 44, pp. 811–818, June 1956.
- [3] H. Fukui, "Available power gain, noise figure, and noise measure of twoports and their graphical representation," *IEEE Trans. Circuit Theory*, vol. CT-13, pp. 137–142, June 1966.
- [4] J. A. Eisenberg, "Systematic design of low-noise, broad band microwave amplifiers using three terminal devices," in *Microwave Semiconductor Devices, Circuits and Applications, Proc. Fourth Cornell Conf.*, 1973, pp. 113–122.
- [5] R. A. Pucel, H. A. Haus, and H. Statz, "Signal and noise properties of gallium arsenide microwave field-effect transistors," in *Advances in Electronics and Electron Physics*. New York: Academic, vol. 38, 1975, pp. 195–265.
- [6] H. Fukui, "The noise performance of microwave transistors," *IEEE Trans. Electron Devices*, vol. ED-13, pp. 329–341, Mar. 1966.
- [7] W. O. Schlosser, private communication.
- [8] B. S. Hewitt *et al.*, "Low-noise GaAs M.E.S.F.E.T.S.," *Electron. Lett.*, vol. 12, pp. 309–310, June 10, 1976.
- [9] "IRE Standards on Electron Tubes: Methods of Testing," 1962, 62 IRE 7 S1, pt. 9: Noise in linear twoports.
- [10] J. Jahncke, "Höchstfrequenzeigenschaften eines GaAs MESFET's in Steifenleitungstechnik," *Nachrichtentechn. Z.*, vol. 5, pp. 193–199, May 1973.
- [11] H. Fukui, "Determination of the basic device parameters of a GaAs MESFET," *Bell Syst. Tech. J.*, vol. 58, pp. 771–797, Mar. 1979.
- [12] B. S. Hewitt *et al.*, "Low-noise GaAs MESFET's: Fabrication and performance," in *Gallium Arsenide and Related Compounds (Edinburgh) 1976, Conf. Series No. 33a*, The Inst. Physics, Bristol and London, 1977, pp. 246–254.
- [13] H. Fukui, "Optimal noise figure of microwave GaAs MESFET's," *IEEE Trans. Electron Devices*, vol. ED-26, pp. 1032–1037, July 1979.
- [14] M. Ogawa, K. Ohata, T. Furutsuka, and N. Kawamura, "Submicron single-gate and dual-gate GaAs MESFET's with improved low noise and high gain performance," *IEEE Trans. Microwave Theory Tech.*, vol. MTT-24, pp. 300–306, June 1976.
- [15] H. F. Cooke, "Microwave field effect transistors in 1978," *Microwave J.*, vol. 21, no. 4, pp. 43–48, Apr. 1978.

# Continuous Varactor-Diode Phase Shifter with Optimized Frequency Response

BENGT ULRIKSSON

**Abstract**—A method is introduced for designing continuous varactor-diode phase shifters with optimum frequency response. The circuit used gives very small frequency variations of the phase shift if the maximum phase shift of the device is less than about 200°. Measurement results on a 180° L-band phase shifter are presented. This unit gives less than 5° variation of any given phase shift less than 180°, when the frequency is changed from 1.5 to 1.7 GHz.

## I. INTRODUCTION

A PROBLEM in the design of continuous varactor-diode phase shifters which has not received previous attention is the optimum frequency behavior at all possible phase shifts. The frequency response is said to be optimum when the derivative of the phase shift with frequency is zero at the center frequency. In this paper the design of a 180° continuous phase shifter will be described, which is almost ideal in this respect.

An interesting 360° varactor-diode phase shifter was introduced in 1971 by Henoch and Tamm [1]. The main parts of the design were two parallel coupled series resonant circuits which were connected to a circulator by means of a quarter-wave transformer. The purpose of the transformer was to equalize the insertion loss. The phase shifter was designed to give optimum frequency behavior at 360° phase shift, but computer simulation has shown large frequency dependence at phase shifts between 0° and 360°.

Starski [2] has reported on an increase in bandwidth for p-i-n-diode reflection-type phase shifters by choosing the length and the impedance of the transformer for optimum frequency response. An attempt was made to improve the continuous 360° shifter in this way, but it was not possible to decrease the frequency variations at all phase shifts to any large extent.

It was, therefore, decided to limit the maximum phase shift to less than 360° by changing one of the series resonant circuits. With an optimized transformer, this circuit has the required performance.

Manuscript received August 2, 1978; revised October 12, 1978.

The author is with the Chalmers University of Technology, Division of Network Theory, Fack, Gothenburg 5, Sweden.

## II. LUMPED ELEMENT PHASE SHIFTER

Fig. 1 shows the phase shifter with lumped elements in the series resonant circuits. The voltage dependence of the series resonant circuits for a phase shifter with less than  $360^\circ$  phase shift is also shown in Fig. 1.

The parameters given are

$Z_c$  impedance of the circulator or the 3-dB hybrid (i.e.,  $50 \Omega$ ),  
 $X, \Gamma$  input reactance and reflection coefficient at the input of the transformer,  
 $Z_T, \Theta_T$  impedance and electrical length of the transformer,  
 $X_L$  total load reactance of the transformer,  
 $X_1, X_2$  reactances of the series resonance circuits,  
 $X_D$  reactance of the diodes.

The phase shift  $\varphi$  of a reflection-type phase shifter can be found from the angle of the reflection coefficient  $\Gamma$  by the following relation:

$$\varphi = \angle \Gamma(V) - \angle \Gamma(V_{\max}), \quad V \in [V_{\min}, V_{\max}]. \quad (1)$$

Optimum frequency response requires that the derivative of the phase shift with frequency should be zero at the center frequency, which gives

$$\frac{\partial \angle \Gamma}{\partial f}(V) = \frac{\partial \angle \Gamma}{\partial f}(V_{\max}), \quad V \in [V_{\min}, V_{\max}]. \quad (2)$$

The angle of the reflection coefficient can be computed from the parameters of the network according to the following set of equations:

$$\angle \Gamma = \pi - 2 \tan^{-1} \left[ \frac{Z_T(X_L \cos \Theta_T + Z_T \sin \Theta_T)}{Z_c(Z_T \cos \Theta_T - X_L \sin \Theta_T)} \right] \quad (3)$$

$$\frac{\partial \angle \Gamma}{\partial f} = - \frac{2Z_c Z_T \left[ Z_T \frac{\partial X_L}{\partial f} + (X_L^2 + Z_T^2) \frac{\Theta_T}{f} \right]}{Z_c^2 [Z_T \cos \Theta_T - X_L \sin \Theta_T]^2 + Z_T^2 [X_L \cos \Theta_T + Z_T \sin \Theta_T]^2} \quad (4)$$

$$X_L = \frac{X_1 X_2}{X_1 + X_2} \quad (5)$$

$$\frac{\partial X_L}{\partial f} = \frac{X_2^2 \frac{\partial X_1}{\partial f} + X_1^2 \frac{\partial X_2}{\partial f}}{(X_1 + X_2)^2} \quad (6)$$

$$X_1 = X_D + 2\pi f L_1 \quad (7)$$

$$X_2 = X_D + 2\pi f L_2 - \frac{1}{2\pi f C}. \quad (8)$$

The inductance  $L_1$  should be chosen so that the reactance  $X_1$  is zero at the maximum voltage

$$X_D(V_{\max}) + 2\pi f L_1 = 0. \quad (9)$$

The components  $L_2$  and  $C$  can now be computed from the requirement that the phase shifter should have a given

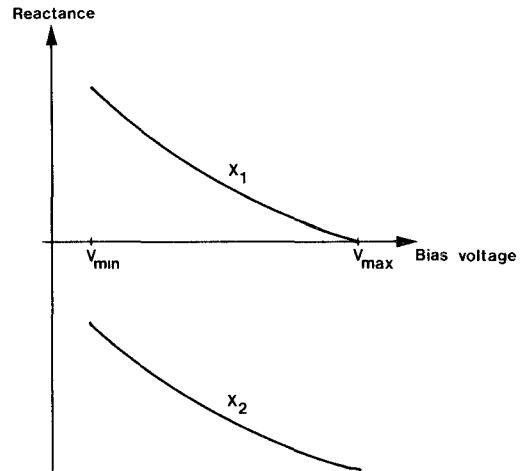
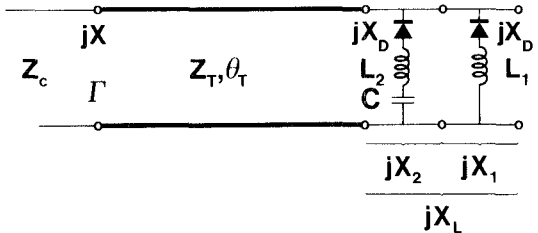


Fig. 1. Lumped-element phase shifter.

maximum phase shift  $\Phi$ , and this maximum phase shift should have optimum frequency response. This means that  $L_2$  and  $C$  can be found for specific values of  $Z_T$  and  $\Theta_T$  from the following equations:

$$\Phi = \angle \Gamma(V_{\min}) - \angle \Gamma(V_{\max}) \quad (10)$$

$$\frac{\partial \angle \Gamma}{\partial f}(V_{\min}) = \frac{\partial \angle \Gamma}{\partial f}(V_{\max}). \quad (11)$$

If (3)–(8) are substituted into (10) and (11), the result is a set of equations from which  $L_2$  and  $C$  can be solved directly. This set of equations has been considerably simplified by the fact that  $X_L(V_{\max})$  is zero according to (9) and (5).

$$X(V_{\min}) = Z_c \tan \left[ \frac{\Phi}{2} + \tan^{-1} \left( \frac{Z_T}{Z_c} \tan \Theta_T \right) \right] \quad (12)$$

$$X_L(V_{\min}) = Z_T \frac{X(V_{\min}) \cos \Theta_T - Z_T \sin \Theta_T}{X(V_{\min}) \sin \Theta_T + Z_T \cos \Theta_T} \quad (13)$$

$$X_2(V_{\min}) = \frac{1}{\frac{1}{X_L(V_{\min})} - \frac{1}{X_1(V_{\min})}} \quad (14)$$

$$\frac{\partial X_2}{\partial f}(V_{\min}) = X_2^2(V_{\min}) \left[ \frac{1}{Z_T X_L^2(V_{\min})} \right] \quad (15)$$

$$L_2 = \frac{\left[ \frac{Z_c^2 [Z_T \cos \Theta_T - X_L(V_{\min}) \sin \Theta_T]^2 + Z_T^2 [X_L(V_{\min}) \cos \Theta_T + Z_T \sin \Theta_T]^2}{Z_T (Z_c^2 \cos^2 \Theta_T + Z_T^2 \sin^2 \Theta_T)} \right.}{\left. \left[ \frac{\partial X_1}{\partial f}(V_{\max}) + Z_T \frac{\Theta_T}{f} \right] - (X_L^2(V_{\min}) + Z_T^2) \frac{\Theta_T}{f} \right] - \frac{1}{X_1^2(V_{\min})} \frac{\partial X_1}{\partial f}(V_{\min}) \quad (16)$$

$$C = \frac{1}{2\pi f(X_D(V_{\min}) + 2\pi f L_2 - X_2(V_{\min}))} \quad (17)$$

The parameters of the transformer ( $Z_T$  and  $\Theta_T$ ) can be used to optimize the frequency behavior at phase shifts which are less than the maximum phase shift  $\Phi$ . This is done by a nonlinear minimization of a variable  $P(Z_T, \Theta_T, \Phi)$ .  $P$  is a measure of the cumulative deviation of phase-frequency slope over the full sweep of phase shift as a function of the design parameters.

$$P(Z_T, \Theta_T, \Phi) = \sum_{n=1}^k \left[ f \cdot \frac{\partial / \Gamma}{\partial f}(V_n) - f \cdot \frac{\partial / \Gamma}{\partial f}(V_{\max}) \right]^2. \quad (18)$$

The voltages  $V_n$  are chosen so that the associated phase shifts  $\varphi(V_n)$  consist of approximately equal steps between zero and  $\Phi$ . A reasonable value for  $k$  is 5.

Since there is no guarantee that  $L_2$  and  $C$  will be realizable (i.e., positive), an efficient steepest descent minimization of (18) will not work properly. Instead a simple step method was used. This means that  $Z_T$  and  $\Theta_T$  were changed with a given step size, and the values of  $Z_T$  and  $\Theta_T$  which gave the smallest value of  $P$  and positive  $L_2$  and  $C$  were kept. The procedure was repeated in the neighborhood of the minimum with a smaller step size until the required accuracy of  $Z_T$  and  $\Theta_T$  was obtained. A short summary of the computer program is given below.

- 1) Compute  $L_1$  from (9).
- 2) Step through  $Z_T$  and  $\Theta_T$  with a given step size.
- 3) For each combination of  $Z_T$  and  $\Theta_T$ , compute  $L_2$  and  $C$  from (12) to (17).
- 4) If  $L_2$  and  $C$  are positive, compute  $P$  from (18). If the value of  $P$  is lower than those previously obtained, keep all parameters.

This program will find the optimum values in about 5–10 min on a normal desk computer (HP 9825).

### III. DISTRIBUTED ELEMENT PHASE SHIFTER

In microwave devices fabricated in stripline it is more convenient to use distributed elements instead of lumped components. Fig. 2 shows the phase shifter with stubs

instead of lumped elements.  $L_1$  has been replaced by a shorted stub, and the  $L_2$ – $C$  combination is replaced by an open stub.

For the shorted stub an equation analogous to (9) is

$$X_D(V_{\max}) + Z_1 \tan \Theta_1 = 0. \quad (19)$$

A shorted stub will always give a larger frequency variation than an inductance. This increase can be minimized by making the impedance of the stub as large as possible. This means that  $Z_1$  should be made as large as possible, and then  $\Theta_1$  can be found from (19).

The parameters of the open stub can be computed from (20) and (21);  $X_2$  and  $(\partial X_2)/(\partial f)$  are given by (14) and (15).

$$X_D - Z_2 \cot \Theta_2 = X_2 \quad (20)$$

$$\frac{\partial X_D}{\partial f} + \frac{Z_2}{\sin^2 \Theta_2} \cdot \frac{\Theta_2}{f} = \frac{\partial X_2}{\partial f}. \quad (21)$$

These are nonlinear equations, but if the equations are slightly rewritten,  $\Theta_2$  can be found by a simple Newton-Raphson iteration, and  $Z_2$  can then be computed directly.

$$\frac{\cos \Theta_2 \cdot \sin \Theta_2}{\Theta_2} = \frac{X_D - X_2}{f \left( \frac{\partial X_2}{\partial f} - \frac{\partial X_D}{\partial f} \right)} \quad (22)$$

$$Z_2 = (X_D - X_2) \tan \Theta_2. \quad (23)$$

Equations (22) and (23) replace (16) and (17) when distributed elements are substituted for lumped elements.

### IV. THEORETICAL RESULTS

Some theoretical results of the continuous phase shifter has been computed for maximum phase shifts from  $90^\circ$  to  $360^\circ$ . In these computations a simple equivalent circuit for the diode was used. This circuit is shown in Fig. 3. The values shown were obtained from measurements on a specific diode (DVH 6730 from Alpha, Inc.) at 1.6 GHz. Diode losses have not been included in the circuit since they do not influence the results. Maximum and minimum voltages for the diode have been chosen as 25 V and 1 V, respectively.

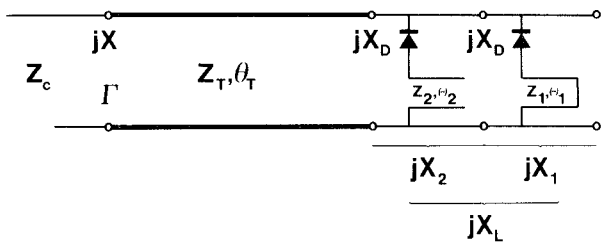


Fig. 2. Phase shifter with distributed elements.

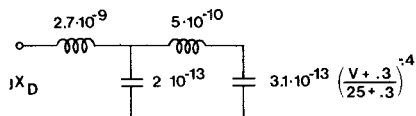
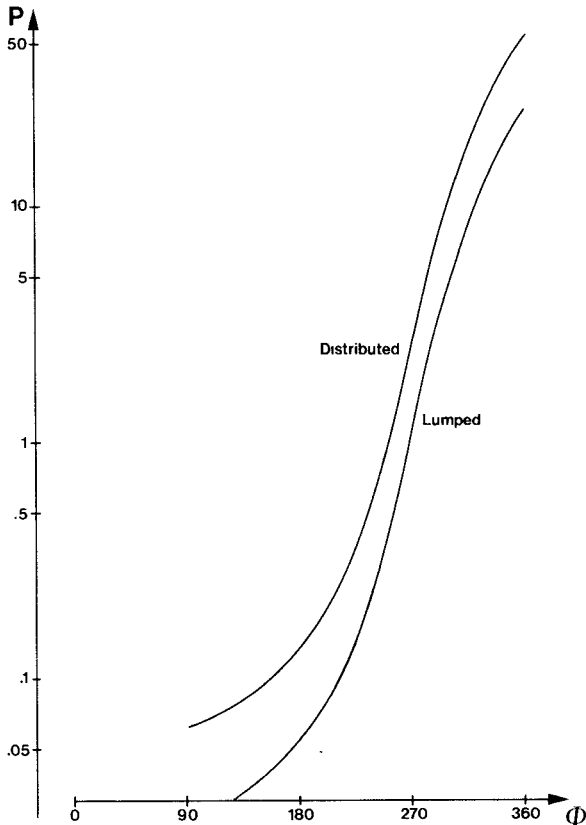


Fig. 3. Equivalent circuit of the diode with measured values.

Fig. 4. Optimum  $P$  as a function of the required maximum phase shift for lumped and distributed phase shifters.  $P$  is a measure of the cumulative deviation of phase-frequency slope for all phase shifts.

In Fig. 4, the optimum  $P$  has been plotted as a function of maximum phase shift for phase shifters with lumped and distributed elements. Fig. 5 gives the maximum total variation of the phase shift over a 7-percent bandwidth (1.5–1.7 GHz) as a function of  $P$ . These values were obtained from complete simulations of the phase shifter with the diode circuit of Fig. 3, and should, therefore, be used with caution when other diodes and other frequency bands are substituted.

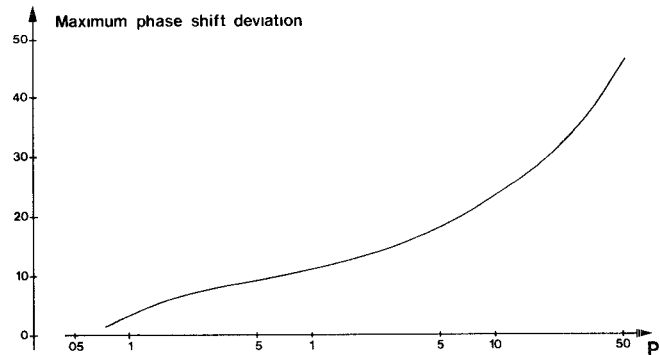
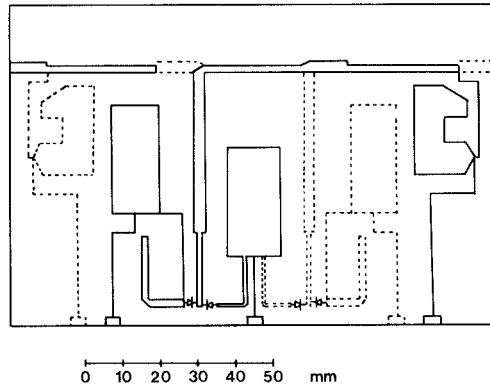
Fig. 5. Maximum variation of the phase shift for frequencies 1.5–1.7 GHz as a function of  $P$ .

Fig. 6. One of the two identical sides of the substrate for the 180° phase shifter; the opposite side is shown as dashed lines.

## V. MEASUREMENT RESULTS

A 180° phase shifter with a center frequency of 1.6 GHz has been fabricated. The following design data were computed.

$$\begin{aligned} Z_1 &= 120 \Omega \\ \Theta_1 &= 54.14^\circ \\ Z_2 &= 86.09 \Omega \\ \Theta_2 &= 66.31^\circ \\ Z_T &= 69.0 \Omega \\ \Theta_T &= 68.0^\circ. \end{aligned}$$

Two identical networks were connected to a 3-dB hybrid of the coupled transmission-line type [3]. This particular hybrid is a broad-side coupled device which is etched on both sides of a 0.381-mm Di-Clad laminate. The Di-Clad is suspended between two 1.59-mm Rexolite 2200 boards.

One side of the Di-Clad laminate is shown as solid lines in Fig. 6. The other side is identical. On the substrate there are also two dc blocks in the form of unloaded 3-dB couplers, and various bias networks. It was found that the length of the shorted stub had to be decreased from the nominal value before a satisfactory result was obtained. The measurement results are shown in Figs. 7–9. Additional values of interest are the maximum input power, which was in the order of 10 mW, and the temperature dependence which was about  $0.1^\circ/\text{°C}$ .

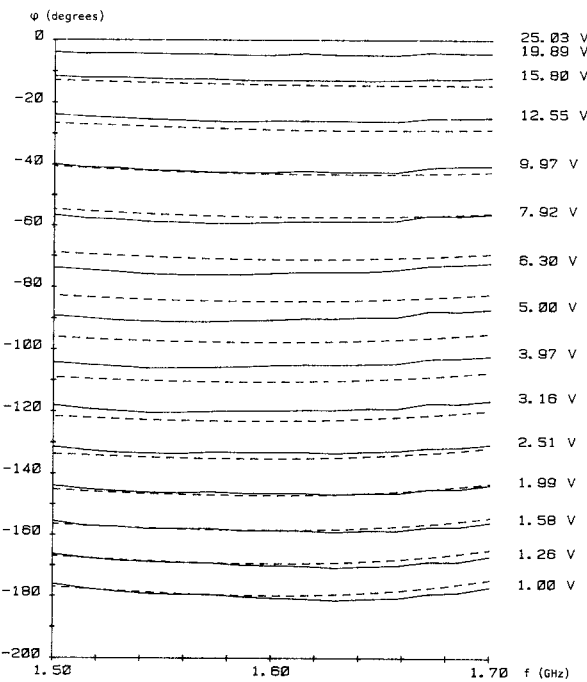


Fig. 7. Phase shift as a function of frequency and bias voltage of the device. The solid lines show measured values and the dashed lines are theoretical results.

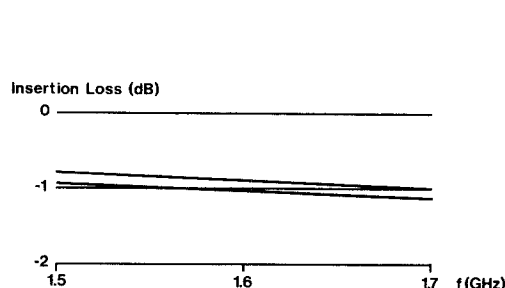


Fig. 8. Measured maximum and minimum insertion loss.

## VI. CONCLUSIONS

A method has been presented which minimizes the frequency dependence at all phase shifts of the continuous varactor-diode phase shifter introduced by Henoch and Tamm [1]. It has also been shown that the frequency variations of the phase shifter can be further decreased by reducing the maximum phase shift. Measurements on a  $180^\circ$  *L*-band phase shifter show close agreement with theory, which predicts a  $\pm 2^\circ$  variation at all phase shifts less than  $180^\circ$  over a 7-percent bandwidth.

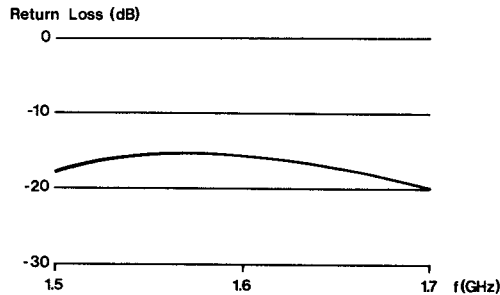


Fig. 9. Measured minimum return loss.

## ACKNOWLEDGMENT

The help and encouragement of Prof. E. Folke Bolinder and Dr. J. Piotr Starski is gratefully acknowledged.

## REFERENCES

- [1] B. T. Henoch and P. Tamm, "A  $360^\circ$  reflection type diode phase modulator," *IEEE Trans. Microwave Theory Tech.*, vol. MTT-19 pp. 103-105, Jan. 1971.
- [2] J. P. Starski, "Optimization of the matching network for a hybrid coupler phase shifter," *IEEE Trans. Microwave Theory Tech.*, vol. MTT-25, pp. 662-666, Aug. 1977.
- [3] —, "Design of *L*-band PIN diode phase shifter," in *Tech. Rep. TR 7801, Chalmers Univ. of Tech., Div. Network Theory*, pp. 8-17, Mar. 1978.